



HAL
open science

Real-time Damper Force Estimation of Vehicle Electrorheological Suspension: A NonLinear Parameter Varying Approach

Thanh-Phong Pham, Olivier Sename, Luc Dugard

► **To cite this version:**

Thanh-Phong Pham, Olivier Sename, Luc Dugard. Real-time Damper Force Estimation of Vehicle Electrorheological Suspension: A NonLinear Parameter Varying Approach. LPVS 2019 - 3rd IFAC Workshop on Linear Parameter Varying Systems, Nov 2019, Eindhoven, Netherlands. 10.1016/j.ifacol.2019.12.354 . hal-02173693

HAL Id: hal-02173693

<https://hal.science/hal-02173693>

Submitted on 4 Jul 2019

HAL is a multi-disciplinary open access archive for the deposit and dissemination of scientific research documents, whether they are published or not. The documents may come from teaching and research institutions in France or abroad, or from public or private research centers.

L'archive ouverte pluridisciplinaire **HAL**, est destinée au dépôt et à la diffusion de documents scientifiques de niveau recherche, publiés ou non, émanant des établissements d'enseignement et de recherche français ou étrangers, des laboratoires publics ou privés.

Real-time Damper Force Estimation of Vehicle Electrorheological Suspension: A NonLinear Parameter Varying Approach^{*}

Thanh-Phong Pham^{*,**} Olivier Sename^{*} Luc Dugard^{*}

^{*} Univ. Grenoble Alpes, CNRS, Grenoble INP[†], GIPSA-lab, 38000 Grenoble, France. [†] Institute of Engineering Univ. Grenoble Alpes (e-mail: thanh-phong.pham2, olivier.sename, luc.dugard@gipsa-lab.grenoble-inp.fr).

^{**} Faculty of Electrical and Electronic Engineering, The University of Danang - University of Technology and Education, 550000 Danang, Vietnam (e-mail: ptphong@ute.udn.vn)

Abstract: This paper proposes a nonlinear parameter varying (*NLPV*) observer to estimate in real-time the damper force of an electrorheological (ER) damper in road vehicle suspension system. First, a nonlinear quarter-car model equipped with the dynamic nonlinear model of ER damper is represented, which captures the main behaviors of the suspension system. The estimation method of the damper force is developed using *NLPV* observer whose objectives are to minimize the effects of bounded unknown road profile disturbances and measurement noises on the estimation errors in the \mathcal{H}_∞ framework. Furthermore, the nonlinearity coming from damper model (and considered in the observer formulation) is handled through a Lipschitz condition. The observer inputs are given by two low-cost sensors data (two accelerometers data from the sprung mass and the unsprung mass). For performance assessment, the observer is implemented on the INOVE testbench from GIPSA-lab (1/5-scaled real vehicle). Both simulation and experimental results demonstrate the effectiveness of proposed observer in terms of the ability of estimating the damper force in real-time and againsting measurement noises and road disturbances.

Keywords: *NLPV* observer, Damping force estimation, Semi-active suspension, Lipschitz condition,

1. INTRODUCTION

Recently, semi-active suspensions are widespread in vehicle applications because of their advantages compared to active and passive suspensions (Savaresi et al. (2010) and references therein). One of the main issues is the control design based on a reduced number of sensors to improve comfort and safety (road holding) for on-board passengers. Therefore, there have been several control methods developed in the literature (see a review in Poussot-Vassal et al. (2012)). Some control approaches are considering the damper force as the control input of the suspension system, then an inverse model or look-up tables are used for implementation (see for instance Poussot-Vassal et al. (2008), Do et al. (2010), Nguyen et al. (2015)). On the other hand, some control design methodologies use an inner force tracking controller in order to attain control objectives (Priyandoko et al. (2009), Aubouet (2010)). Therefore, the damper force signal is crucial for control and diagnosis of suspension systems.

Some methodologies were developed to estimate the damper force, since the damper force sensors are difficult

and expensive setup in practice. The key challenges for designing this estimation are to reduce the cost of the required sensors, to take the dynamic behavior of damper into account and to deal with the nonlinearity. Along the line of research for the damper force estimation, some contributions have been proposed in literature as follows:

- The work by Koch et al. (2010) presented the Kalman filters to estimate the damper force but ignores the dynamic characteristic of the semi-active damper.
- The authors have proposed several works in that context:
 - (1) Estrada-Vela et al. (2018) and Pham et al. (2018) proposed H_∞ and H_2 damping force observers based on a dynamic nonlinear model of the ER damper, while three sensors are required as inputs of the observer.
 - (2) Tudon-Martinez et al. (2018) introduced an LPV- H_∞ filter for estimating the damper force based on deflection and deflection velocity data, which are difficult and expensive to be measured.
 - (3) Pham et al. (2019) proposed an H_∞ observer using two accelerometers to estimate the damper force in the ER suspension system while the nonlinearity in the ER damper model is bounded by Lipschitz condition. However, the variation of

^{*} This work has been partially supported by the 911 scholarship from Vietnamese government. The authors also thank the financial support of the ITEA 3, 15016 EMPHYSIS project.

the the damper force amplification function of the voltage input were not considered in the design step.

To handle this issue, an *NLPV* observer is proposed here where the observer gain depends on the voltage control input u . The proposed method considers two accelerometers (sprung mass and unsprung mass accelerations) as inputs of observer. The design of the observer is based on a nonlinear suspension model made of a quarter-car vehicle model, augmented with a first order dynamical nonlinear damper model, which captures the main behavior of the ER dampers in an automotive application. It is worth noting that the damper nonlinearity is multiplied by the control input u ; therefore, the latter will be considered as a scheduling parameter. Then a *NLPV* observer is developed bounding the nonlinearity by a Lipschitz condition and minimizing the effect of unknown input disturbances (road profile derivative and measurement noises) on the estimation errors via \mathcal{H}_∞ framework.

The major contributions of this paper are as follows:

- A *NLPV* approach for Lipschitz nonlinear system is developed to design a damper force observer minimizing, in an \mathcal{L}_2 -induced gain objective, the effect of unknown inputs (road profile and measurement noises).
- The proposed observer has been implemented on a real scaled-vehicle test bench, through the Matlab/Simulink real-time workshop. The observer performances are then assessed with experimental tests

The rest of this paper is as follows. Section 2 presents the dynamic of quarter car system and the *NLPV* reformulation. Section 3 provides the design of *NLPV* observer. In section 4 this method is analyzed in frequency and time domain simulation. Section 5 discusses the experimental results and finally, section 6 give some concluding remarks.

2. SEMI-ACTIVE SUSPENSION MODELING AND QUARTER-CAR SYSTEM DESCRIPTION

2.1 Semi-active suspension modeling

First a nonlinear dynamical model of semi-active ER suspension is expressed as

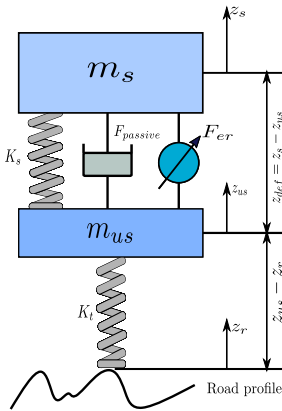


Fig. 1. 1/4 car model with semi-active suspension

$$\begin{cases} F_d &= k_0(z_s - z_{us}) + c_0(\dot{z}_s - \dot{z}_{us}) + F_{er} \\ \dot{F}_{er} &= -\frac{1}{\tau}F_{er} + \frac{f_c}{\tau} \cdot u \cdot \tanh(k_1(z_s - z_{us})) \\ &+ c_1(\dot{z}_s - \dot{z}_{us}) \end{cases} \quad (1)$$

where F_d is the damper force; $c_0, c_1, k_0, k_1, f_c, \tau$ are constant parameters; z_s and z_{us} are the displacements of the sprung and unsprung masses, respectively. The control input u is the voltage input that provides the electrical field to control the ER damper. In practice, it is the duty cycle of the PWM signal that controls the application (shown in table 2).

Remark 1: It is worth noting that if time constant τ is zero, the model (1) becomes Guo's model (see Guo et al. (2006))

To determine the parameters of the above model, linear and nonlinear identification methodologies were used (shown in table 1). They are not described here since it is out of the scope of this paper.

Table 1. Parameter values of the quarter-car model equipped with an ER damper

Parameter	Description	value	Unit
m_s	Sprung mass	2.27	kg
m_{us}	unsprung mass	0.25	kg
k_s	Spring stiffness	1396	N/m
k_t	Tire stiffness	12270	N/m
k_0	Passive damper stiffness coefficient	170.4	N/m
c_0	Viscous damping coefficient	68.83	N.s/m
k_1	Hysteresis coefficient due to displacement	218.16	N.s/m
c_1	Hysteresis coefficient due to velocity	21	N.s/m
f_c	Dynamic yield force of ER fluid	28.07	N
τ	Time constant	43	ms

Table 2. Range of control input value u

Control input	Description	value
u	Duty cycle of PWM channel	[0, 1]

2.2 Quarter-car system description

This section introduces the quarter-car model with the semi-active ER suspension system depicted in Fig.1. The well-known model consists of the sprung mass (m_s), the unsprung mass (m_{us}), the suspension components located between (m_s) and (m_{us}) and the tire which is modelled as a spring with stiffness k_t . From Newton's second law of motion, the system dynamics around the equilibrium are given as:

$$\begin{cases} m_s \ddot{z}_s &= -F_s - F_d \\ m_{us} \ddot{z}_{us} &= F_s + F_d - F_t \end{cases} \quad (2)$$

where $F_s = k_s(z_s - z_{us})$ is the spring force; $F_t = k_t(z_{us} - z_r)$ is the tire force; the damper force F_d is given as in (1). z_s and z_{us} are the displacements of the sprung and unsprung masses, respectively; z_r is the road displacement input.

By selecting the system states as $x = [x_1, x_2, x_3, x_4, x_5]^T = [z_s - z_{us}, \dot{z}_s, z_{us} - z_r, \dot{z}_{us}, F_{er}]^T \in \mathbb{R}^5$, the measured variables $y = [\ddot{z}_s, \ddot{z}_{us}]^T \in \mathbb{R}^2$, the variables to be estimated $z = [x_1, x_2, x_4, x_5]^T \in \mathbb{R}^4$ and the scheduling variable

$\rho = u \in \mathbb{R}$ (Table 2), the system dynamics can be written in the following NLPV form:

$$\begin{cases} \dot{x} &= Ax + B(\rho)\Phi(x) + D_1\omega \\ y &= Cx + D_2\omega \\ z &= C_zx \end{cases} \quad (3)$$

where

$\omega = \begin{pmatrix} \dot{z}_r \\ n \end{pmatrix}$, in which, \dot{z}_r is the road profile derivative and n is the sensor noises.

$$\begin{aligned} \Phi(x) &= \tanh(k_1x_1 + c_1(x_2 - x_4)) \\ &= \tanh(\Gamma x) \end{aligned}$$

with $\Gamma = [k_1, c_1, 0, -c_1, 0]$

Therefore, $\Phi(x)$ satisfies the Lipschitz condition in x

$$\|\Phi(x) - \Phi(\hat{x})\| \leq \|\Gamma(x - \hat{x})\|, \forall x, \hat{x} \quad (4)$$

$$A = \begin{bmatrix} 0 & 1 & 0 & -1 & 0 \\ -\frac{(k_s + k_0)}{m_s} & -\frac{c_0}{m_s} & 0 & \frac{c_0}{m_s} & -\frac{1}{m_s} \\ 0 & 0 & 0 & 1 & 0 \\ \frac{(k_s + k_0)}{m_{us}} & \frac{c_0}{m_{us}} & -\frac{k_t}{m_{us}} & -\frac{c_0}{m_{us}} & \frac{1}{m_{us}} \\ 0 & 0 & 0 & 0 & -\frac{1}{\tau} \end{bmatrix}$$

$$C = \begin{bmatrix} -\frac{(k_s + k_0)}{m_s} & -\frac{c_0}{m_s} & 0 & \frac{c_0}{m_s} & -\frac{1}{m_s} \\ \frac{(k_s + k_0)}{m_{us}} & \frac{c_0}{m_{us}} & -\frac{k_t}{m_{us}} & -\frac{c_0}{m_{us}} & \frac{1}{m_{us}} \end{bmatrix}$$

$$B = \begin{bmatrix} 0 \\ 0 \\ 0 \\ \frac{f_c}{\tau} \rho \end{bmatrix}, C_z = \begin{bmatrix} 1 & 0 & 0 & 0 & 0 \\ 0 & 1 & 0 & 0 & 0 \\ 0 & 0 & 0 & 1 & 0 \\ 0 & 0 & 0 & 0 & 1 \end{bmatrix}, D_1 = \begin{bmatrix} 0 & 0 \\ 0 & 0 \\ -1 & 0 \\ 0 & 0 \\ 0 & 0 \end{bmatrix}$$

$$D_2 = \begin{bmatrix} 0 & 0.01 \\ 0 & 0.01 \end{bmatrix}$$

According to Apkarian et al. (1995), since the matrix $B(\rho)$ is affine in ρ and since the scheduling parameter ρ varies in a polytope \mathcal{Y} of 2 vertices $\rho \in [\rho, \bar{\rho}]$, it can be transformed into a convex interpolation as follows:

$$B(\rho) = \sum_{i=1}^2 \alpha_i(\rho)B_i, \quad \alpha_i(\rho) \geq 0, \quad \sum_{i=1}^2 \alpha_i(\rho) = 1 \quad (5)$$

where $B_1 = B(\rho)$, $B_2 = B(\bar{\rho})$

Note that the measured outputs $y = [\dot{z}_s, \dot{z}_{us}]^T$ can be obtained easily from on board sensors (accelerometers) and the scheduling variable $\rho = u$ are real-time accessible.

3. NLPV OBSERVER DESIGN

In this section, a NLPV observer is proposed to estimate the ER damper force accurately. The unknown input ω (road profile disturbance and measurement noise) is considered as an unknown disturbance. Therefore, a H_∞ criterion is used to minimize the effect of the unknown disturbance ω on the state estimation errors and to bound the nonlinearity by Lipschitz constant.

The NLPV observer for the quarter-car system (3) is chosen as:

$$\begin{cases} \dot{\hat{x}} &= A\hat{x} + L(\rho)(y - C\hat{x}) + B(\rho)\Phi(\hat{x}) \\ \hat{z} &= C_z\hat{x} \end{cases} \quad (6)$$

where \hat{x} is the estimated states vector of x , \hat{z} represents the estimated variables of the variables z . The observer gain $L(\rho)$ to be determined in the next steps is defined as follows:

$$L(\rho) = \sum_{i=1}^2 \alpha_i(\rho)L_i \quad (7)$$

with $L_i \in \mathbb{R}^{5 \times 2}$

The estimation error is given as

$$e(t) = x(t) - \hat{x}(t) \quad (8)$$

Differentiating $e(t)$ with respect to time and using (3) and (6), one obtains

$$\begin{cases} \dot{e} &= \dot{x} - \dot{\hat{x}} \\ &= Ax + B(\rho)\Phi(x) + D_1\omega \\ &\quad - A\hat{x} - L(\rho)(y - C\hat{x}) - B\Phi(\hat{x}) \\ &= (A - L(\rho)C)e + B(\rho)(\Phi(x) - \Phi(\hat{x})) \\ &\quad + (D_1 - L(\rho)D_2)\omega \\ e_z &= C_z e \end{cases} \quad (9)$$

The problem to be solved then is stated as:

- The system (9) is stable for $\omega(t) = 0$
- Minimize γ such that $\|e_z(t)\|_{\mathcal{L}_2} < \gamma\|\omega(t)\|_{\mathcal{L}_2}$ for $\omega(t) \neq 0$

The following theorem solves the above problem into an LMI framework.

Theorem 1. Consider the system model (3) and the observer (6). The above design problem is solved if there exist a symmetric positive definite matrix P , a matrix Y_i with $i = 1, 2$ and positive scalar ϵ_i minimizing γ such that:

$$\begin{bmatrix} \Omega_i & PB_i & PD_1 + Y_i D_2 \\ * & -\epsilon_i I_d & 0_{n,d} \\ * & * & -\gamma^2 I \end{bmatrix} < 0 \quad (10)$$

where $\Omega_i = A^T P + PA + Y_i C + C^T Y_i^T + \epsilon_i \Gamma^T \Gamma + C_z^T C_z$

the observer vertex matrices are $L_i = -P^{-1}Y_i$

Proof. Consider the following Lyapunov function

$$V(t) = e(t)^T P e(t) \quad (11)$$

Differentiating $V(t)$ along the solution of (9) yields

$$\begin{aligned} \dot{V}(t) &= \dot{e}(t)^T P e(t) + e(t)^T P \dot{e}(t) \\ &= [(A - L(\rho)C)e + B(\rho)(\Phi(x) - \Phi(\hat{x})) \\ &\quad + (D_1 - L(\rho)D_2)\omega]^T P e + e^T P [(A - L(\rho)C)e \\ &\quad + B(\rho)(\Phi(x) - \Phi(\hat{x})) + (D_1 - L(\rho)D_2)\omega] \end{aligned} \quad (12)$$

Defining $\eta = \begin{bmatrix} e \\ \Phi(x) - \Phi(\hat{x}) \\ \omega \end{bmatrix}$, one obtains

$$\dot{V}(t) = \eta^T M \eta \quad (13)$$

where

$$M = \begin{bmatrix} \Omega_1(\rho) & PB(\rho) & P(D_1 - L(\rho)D_2) \\ B(\rho)^T P & 0 & 0 \\ (D_1 - L(\rho)D_2)^T P & 0 & 0 \end{bmatrix} \text{ with}$$

$$\Omega_1(\rho) = (A - L(\rho)C)^T P + P(A - L(\rho)C)$$

From (4), the following condition is obtained

$$\begin{aligned} (\Phi(x) - \Phi(\hat{x}))^T (\Phi(x) - \Phi(\hat{x})) &\leq e^T \Gamma^T \Gamma e \\ \Leftrightarrow \eta^T Q \eta &\leq 0 \end{aligned} \quad (14)$$

$$\text{where } Q = \begin{bmatrix} -\Gamma^T \Gamma & 0 & 0 \\ 0 & I & 0 \\ 0 & 0 & 0 \end{bmatrix}$$

In order to satisfy the objective design w.r.t. the \mathcal{L}_2 gain disturbance attenuation, the \mathcal{H}_∞ performance index is defined as:

$$\begin{aligned} J &= e_z^T e_z - \gamma^2 \omega^T \omega \\ &= \eta^T R \eta \end{aligned} \quad (15)$$

$$\text{where } R = \begin{bmatrix} C_z^T C_z & 0 & 0 \\ 0 & 0 & 0 \\ 0 & 0 & -\gamma^2 I \end{bmatrix}$$

By applying the \mathcal{S} -procedure (Boyd et al. (1994)) to both constraints (14) and $J \geq 0$, $\dot{V}(t) < 0$ if there exists a scalar $\epsilon_l > 0$ such that

$$\begin{aligned} \dot{V}(t) - \epsilon_l (\eta^T Q \eta) + J &< 0 \\ \Leftrightarrow \eta^T (M - \epsilon_l Q + R) \eta &< 0 \end{aligned} \quad (16)$$

The condition (16) is equivalent to

$$\begin{aligned} M - \epsilon_l Q + R &< 0 \\ \Leftrightarrow \begin{bmatrix} \Omega_1(\rho) + \epsilon_l \Gamma^T \Gamma + C_z^T C_z & PB(\rho) & P(D_1 - L(\rho)D_2) \\ B(\rho)^T P & -\epsilon_l I & 0 \\ (D_1 - L(\rho)D_2)^T P & 0 & -\gamma^2 I \end{bmatrix} &< 0 \end{aligned} \quad (17)$$

Let define $Y_i = -PL_i$ and substitute (5), (7) into (17), the LMI (10) is obtained.

If (10) is satisfied and since the term $\epsilon_l (\eta^T Q \eta) \leq 0$, one obtains

$$\begin{aligned} \dot{V} + J &< 0 \\ \Leftrightarrow \dot{V} &< \gamma^2 \omega^T \omega - e_z^T e_z \end{aligned} \quad (18)$$

By integrating the both sides of (18), one obtains (Darouach et al. (2011))

$$\begin{aligned} \int_0^\infty \dot{V}(\tau) d\tau &< \int_0^\infty \gamma^2 \omega(\tau)^T \omega(\tau) d\tau - \int_0^\infty e_z(\tau)^T e_z(\tau) d\tau \\ \Leftrightarrow V(\infty) - V(0) &< \gamma^2 \|\omega(t)\|_{\mathcal{L}_2}^2 - \|e_z(t)\|_{\mathcal{L}_2}^2 \end{aligned} \quad (19)$$

Under zero initial conditions, (19) becomes

$$V(\infty) < \gamma^2 \|\omega(t)\|_{\mathcal{L}_2}^2 - \|e_z(t)\|_{\mathcal{L}_2}^2 \quad (20)$$

It is equivalent to

$$\|e_z(t)\|_{\mathcal{L}_2}^2 < \gamma^2 \|\omega(t)\|_{\mathcal{L}_2}^2 \quad (21)$$

The proof of Theorem 1 is completed. \square

4. ANALYSIS OF THE OBSERVER DESIGN: FREQUENCY AND TIME DOMAIN SIMULATIONS

In this section, the synthesis result of the *NLPV* observer is shown and some simulation scenarios are considered. The proposed observer is applied to the system presented

in section 2. It is worth noting that for INOVE testbed available at GIPSA-lab, the control input u (duty cycle of PWM signal) is limited in the range of $[0, 1]$ (see Table 2)

4.1 Synthesis results and frequency domain analysis

Solving Theorem 1 with $\underline{\rho} = 0$ and $\bar{\rho} = 1$, we obtain the minimum \mathcal{L}_2 -induced gain $\gamma = 1.0001$, $\epsilon_l = 4$ and the observer gains

$$L_1 = \begin{bmatrix} -3.4572 & -0.0015 \\ -3.7771 & -0.0022 \\ -5.1680 & -4.8398 \\ -0.4777 & 0.9998 \\ 107.9617 & -0.9147 \end{bmatrix}$$

$$L_2 = \begin{bmatrix} -3.4397 & -0.0015 \\ -3.7503 & -0.0022 \\ -5.1910 & -4.8392 \\ -0.4750 & 0.9998 \\ 42.2868 & 0.0204 \end{bmatrix}$$

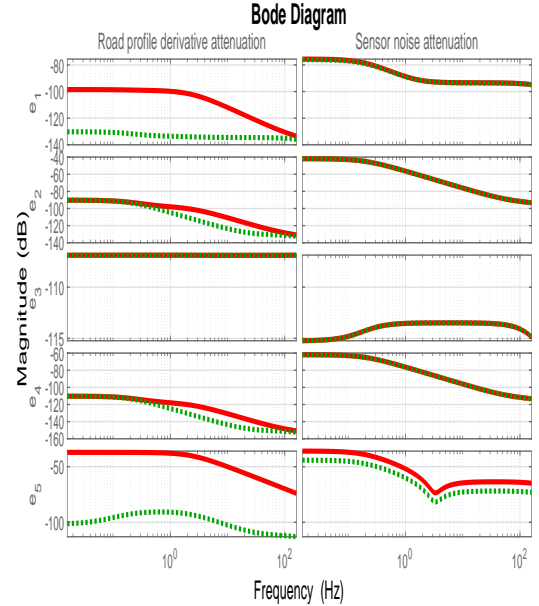


Fig. 2. Transfer $\|e_z/\omega\|$ - Bode diagrams of *NLPV* observer with $\rho = 0$ (red solid) and *NLPV* observer with $\bar{\rho} = 1$ (green dash), w.r.t road profile derivative (left) and w.r.t measurement noise (right).

In Figure 2 the Bode diagrams of the estimation error systems with input ω (road profile derivative and sensor noise) and output (the state estimation errors) are shown for the frozen values of the parameter $\rho = \{0, 1\}$. These results emphasize the satisfactory attenuation level of unknown road profile derivative and measurement noises effect on the 4 estimation errors e_z with scheduling parameter $\rho = \underline{\rho} = 0$ (red line) and $\rho = \bar{\rho} = 1$ (green dash).

4.2 Time-domain simulation

To emphasize the effectiveness of the proposed approach, simulations are now performed considering the nonlinear quarter-car model (3).

The initial conditions of the proposed design are as follows: $x_0 = [0, 0, 0, 0, 0]^T$, $\hat{x}_0 = [0.01, -0.1, 0.001, -0.1, 5]^T$

Four simulation scenarios are used to evaluate the performance of the observer as follows:

Scenario 1: Test with various road frequencies

- The road profile is a chirp signal
- The control input u is constant ($u = 0.3$)

Scenario 2: Test with a slow varying of scheduling parameter

- An ISO 8608 road profile signal (Type C) is used.
- The control input is sin wave with low frequency

Scenario 3: Test the stability of the *NLPV* observer with a step road profile

- A step road profile is used.
- Control input u is obtained from a Skyhook controller

Scenario 4: Test of the *NLPV* observer for a closed-loop system with an infinitely fast varying scheduling parameter

- An ISO 8608 road profile signal (Type C) is used.
- Control input u is obtained from a Skyhook controller

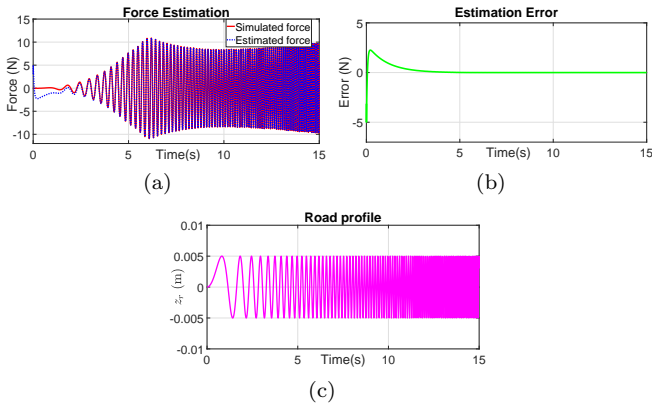


Fig. 3. Simulation scenario 1 ($\rho = u = 0.3$): (a) Damping force estimation, (b) Estimation error, (c) Road profile

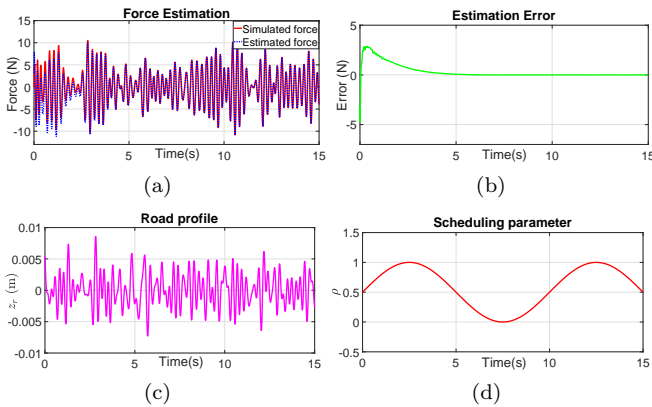


Fig. 4. Simulation scenario 2: (a) Damping force estimation, (b) Estimation error, (c) Road profile (d) Scheduling parameter

The simulation results of four tests are shown in the Fig. 3, Fig. 4, Fig 5 and Fig. 6. According to Fig. 3, the robustness of *NLPV* observer to the frequency of road profile disturbance are guaranteed. It can be clearly observed in Fig. 3b that the damping force is estimated with a satisfactory accuracy at all of frequencies of road profile. In Fig. 4, the performance of the proposed observer is assessed in case of slow varying of scheduling parameter. Fig 5 demonstrates the stability of proposed observer with a step road profile (road profile derivative value is very large) Fig. 6 illustrated the robustness of the proposed *LPV* observer when scheduling parameter varies infinitely fast.

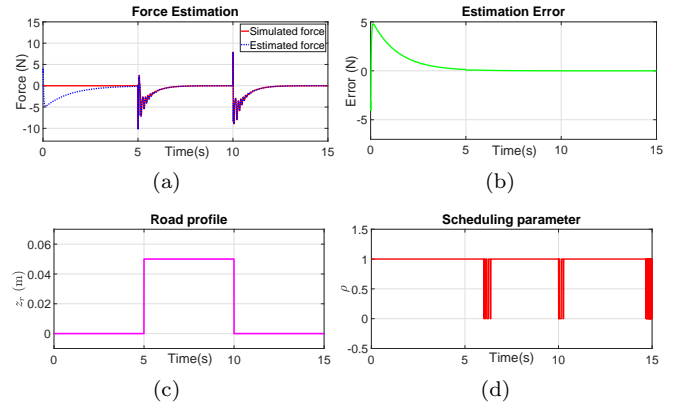


Fig. 5. Simulation scenario 3: (a) Damping force estimation, (b) Estimation error, (c) Road profile, (d) Scheduling parameter

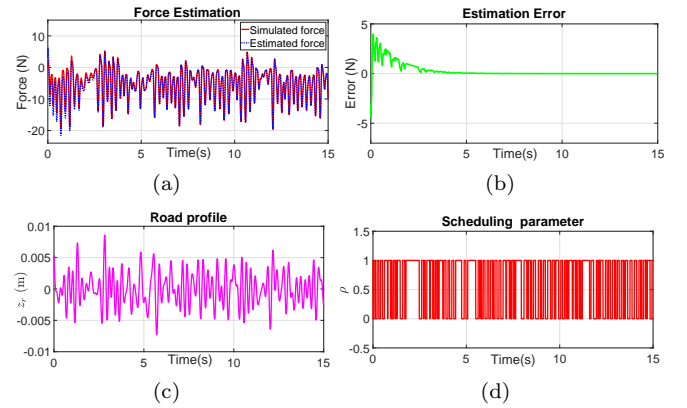


Fig. 6. Simulation scenario 3: (a) Damping force estimation, (b) Estimation error, (c) Road profile (d) Scheduling parameter

5. EXPERIMENTAL VALIDATION

To validate the effectiveness of the proposed algorithm in a real situation, experiments have been performed on the 1/5 car scaled car INOVE available at GIPSA-lab, shown in Fig. 7.



Fig. 7. The experimental testbed INOVE at GIPSA-lab (see www.gipsa-lab.fr/projet/inove)

This test-bench which involves 4 semi-active ER suspensions is controlled in real-time using xPC target and a host computer. The target PC is connected to the host computer via Ethernet communication standard. The proposed observer system is implemented on the host PC using Matlab/simulink. Note that the experimental platform is fully equipped sensors to measure its vertical motion. Each corner of the system has a DC motor to generate the road profile.

In this study, the proposed algorithm is applied for the rear-left corner. As previously mentioned, only both unsprung mass acceleration \ddot{z}_{us} and sprung mass acceleration \ddot{z}_s are used as inputs of the proposed observer. For validation purpose only, the damper force sensor is used to compare the measured force with the estimated one. The following block-scheme illustrates the experiment procedure of the estimation (see Fig. 8).

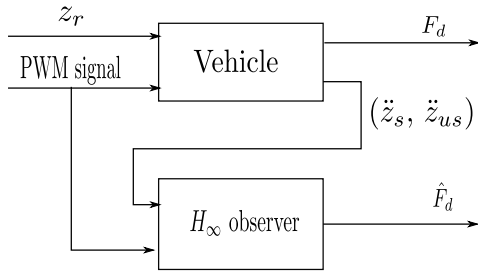


Fig. 8. Block diagram for implementation of the \mathcal{H}_∞ damper force observer

Two experimental scenarios are shown below:

Experiment 1:

- The road profile is sequence of sinusoidal bumps
- The control input u is obtained from a Skyhook controller

Experiment 2:

- An ISO 8608 road profile signal (Type C) is used.
- The control input u is obtained from a Skyhook controller

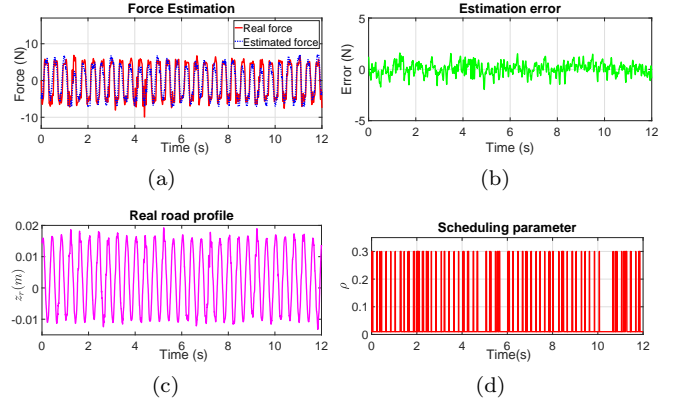


Fig. 9. Experiment 1: (a) Damping force estimation, (b) Estimation error, (c) Road profile (d) Scheduling parameter

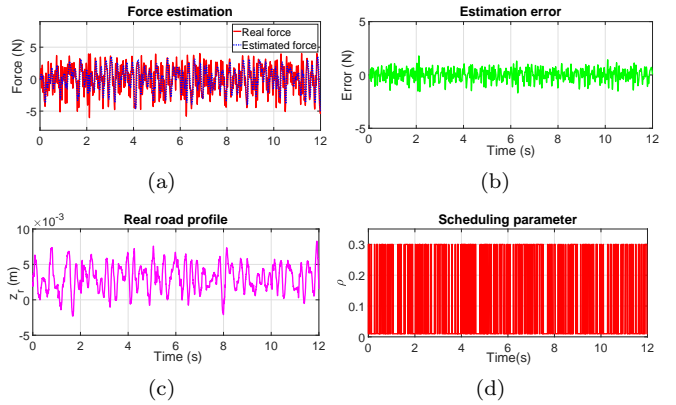


Fig. 10. Experiment 2: (a) Damping force estimation, (b) Estimation error, (c) Road profile (d) Scheduling parameter

Table 3. Normalized Root-Mean-Square Errors (NRMSE)

Road Profile	NRMSE
Experiment 1	0.1125
Experiment 2	0.1342

Fig. 9 and Fig. 10 are the experiment results of the observer in experimental scenario 1 and 2, respectively. The results demonstrate the accuracy and efficiency of the proposed observer in realistic tests. To further describe this accuracy, Table 3 presents the normalized root-mean-square errors w.r.t. maximum value, considering the difference between the estimated and measured forces in experiment 1 and experiment 2.

6. CONCLUSION

This paper presented a *NLPV* observer to estimate the damper force, using the dynamic nonlinear model of the ER damper. For this purpose, the quarter-car system is represented in a *NLPV* form by considering a phenomenological model of damper for which the nonlinearity term bounded by a Lipschitz condition. Based on two accelerometers, a *NLPV* observer is designed, giving good

estimation results of the damping force. The estimation error is minimized accounting for the effect of unknown inputs (road profile derivative and measurement noises). Both simulation and experiment results assess the ability and the accuracy of the proposed models to estimate the damping force of the ER semi-active damper.

REFERENCES

- Apkarian, P., Gahinet, P., and Becker, G. (1995). Self-scheduled h_∞ control of linear parameter-varying systems: a design example. *Automatica*, 31(9), 1251–1261.
- Aubouet, S. (2010). *Semi-active SOBEN suspensions modeling and control*. Ph.D. thesis, Institut National Polytechnique de Grenoble-INPG.
- Boyd, S., El Ghaoui, L., Feron, E., and Balakrishnan, V. (1994). *Linear matrix inequalities in system and control theory*, volume 15. Siam.
- Darouach, M., Boutat-Baddas, L., and Zerrougui, M. (2011). h_∞ observers design for a class of nonlinear singular systems. *Automatica*, 47(11), 2517–2525.
- Do, A.L., Sename, O., and Dugard, L. (2010). An lpv control approach for semi-active suspension control with actuator constraints. In *American Control Conference (ACC), 2010*, 4653–4658. IEEE.
- Estrada-Vela, A., Alcántara, D.H., Menendez, R.M., Sename, O., and Dugard, L. (2018). h_∞ observer for damper force in a semi-active suspension. *IFAC-PapersOnLine*, 51(11), 764–769.
- Guo, S., Yang, S., and Pan, C. (2006). Dynamic modeling of magnetorheological damper behaviors. *Journal of Intelligent material systems and structures*, 17(1), 3–14.
- Koch, G., Kloiber, T., and Lohmann, B. (2010). Nonlinear and filter based estimation for vehicle suspension control. In *Decision and Control (CDC), 2010 49th IEEE Conference on*, 5592–5597. IEEE.
- Nguyen, M.Q., da Silva, J.G., Sename, O., and Dugard, L. (2015). Semi-active suspension control problem: Some new results using an lpv/ h_∞ state feedback input constrained control. In *Decision and Control (CDC), 2015 IEEE 54th Annual Conference on*, 863–868. IEEE.
- Pham, T.P., Sename, O., and Dugard, L. (2019). Design and Experimental Validation of an H_∞ Observer for Vehicle Damper Force Estimation. In *9th IFAC International Symposium on Advances in Automotive Control (AAC 2019)*. Orléans, France.
- Pham, T.P., Sename, O., Dugard, L., and Vu, V.T. (2018). Real-time estimation of the damping force of vehicle electrorheological suspension. In *VSDIA 2018 - The 16th Mini Conference on Vehicle System Dynamics, Identification and Anomalies*. Budapest, Hungary.
- Poussot-Vassal, C., Sename, O., Dugard, L., Gaspar, P., Szabo, Z., and Bokor, J. (2008). A new semi-active suspension control strategy through lpv technique. *Control Engineering Practice*, 16(12), 1519–1534.
- Poussot-Vassal, C., Spelta, C., Sename, O., Savaresi, S.M., and Dugard, L. (2012). Survey and performance evaluation on some automotive semi-active suspension control methods: A comparative study on a single-corner model. *Annual Reviews in Control*, 36(1), 148–160.
- Priyandoko, G., Mailah, M., and Jamaluddin, H. (2009). Vehicle active suspension system using skyhook adaptive neuro active force control. *Mechanical systems and signal processing*, 23(3), 855–868.
- Savaresi, S.M., Poussot-Vassal, C., Spelta, C., Sename, O., and Dugard, L. (2010). *Semi-active suspension control design for vehicles*. Elsevier.
- Tudon-Martinez, J.C., Hernandez-Alcantara, D., Sename, O., Morales-Menendez, R., and de J. Lozoya-Santos, J. (2018). Parameter-dependent h_∞ filter for lpv semi-active suspension systems. volume 51, 19–24. Elsevier.